

Microstructure of Stircast Al-Pb Metal-Metal Composites

S. Mohan*, V. Agarwala** and S. Ray**

*Department of Metallurgical Engineering, Institute of Technology, Banaras Hindu University, Varanasi-221005, India

**Department of Metallurgical Engineering, University of Roorkee, Roorkee-247 667, India

Stircast Al-Pb Metal-Metal composites have been produced at a high rotational speed of 53 s^{-1} with different lead contents and with the same lead content but different rotational speeds of 53, 37 and 25 s^{-1} in a stircasting unit with facilities for bottom pouring and rapid solidification. Microstructure, particle size distribution and inter-particle distance have been determined by optical and scanning electron microscopy in order to see the effect of lead content and agitator speed. It has been observed that the microstructure of stircast composite is influenced significantly both by lead content and agitator speed during casting.

(Received March 2, 1992)

Keywords: stircast, aluminium-lead alloy, composite, metal-metal composite

I. Introduction

In recent years, use of aluminium-base bearing materials has increased especially in automobile industries⁽¹⁾ due to their light weight. Among aluminium base materials, Al-Pb metal-metal composites have given an attractive alternative to most commonly used Al-Sn alloys⁽¹⁾⁻⁽³⁾.

However, problems arise in the production of Al-Pb composite due to negligible mutual solubility and wide miscibility gap resulting in severe gravity segregation of lead because of large difference in density between aluminium and lead. Therefore, it is almost impossible to disperse lead in aluminium uniformly to the desired extent by conventional melting and casting techniques. Several techniques have been developed to overcome the above problems⁽¹⁾⁻⁽⁴⁾. But it is very expensive to produce Al-Pb composites either by powder metallurgy or space metallurgy and in the case of conventional rapid solidification, the microstructure of the alloy in the centre differs from that of surface of the ingot. Ichikawa *et al.*⁽⁴⁾ produced the rheocast Al-Pb composite at a high rotational speed of 70 s^{-1} under vacuum. Microstructures show a lead-rich phase along the boundaries of the primary aluminium phase.

The objective of the present investigation is to develop a stircast Al-Pb composite with high rotational speed and to study the effect of lead content on the microstructure.

II. Experimental Procedure

Table 1 shows the chemical composition, stirring speed, density and porosity of the composite synthesized for the current investigation. Figure 1 shows the experimental set-up used for the study. The desired amount of the commercially pure aluminium was charged into a

Table 1 Composition, agitator speed, density and porosity of stircast Al-Pb metal-metal composite.

Stirring speed, (s^{-1})	Chemical analysis mass%	sp. gravity	Porosity (vol%)
53	3.69Pb 0.74Fe 0.05Si Rest Al	2.50	10.07
53	8.04Pb 0.70Fe 0.05Si Rest Al	2.58	10.42
53	10.39Pb 0.69Fe 0.05Si Rest Al	2.61	10.92
53	20.09Pb 0.61Fe 0.05Si Rest Al	2.83	11.29
53	30.18Pb 0.53Fe 0.04Si Rest Al	3.10	11.68
53	47.56Pb 0.40Fe 0.03Si Rest Al	3.77	10.87
53	55.83Pb 0.34Fe 0.03Si Rest Al	4.22	10.21
53	9.24Pb 0.69Fe 0.05Si Rest Al	2.62	9.66
37	9.20Pb 0.67Fe 0.05Si Rest Al	2.60	10.34
25	9.18Pb 0.68Fe 0.05Si Rest Al	2.63	9.31

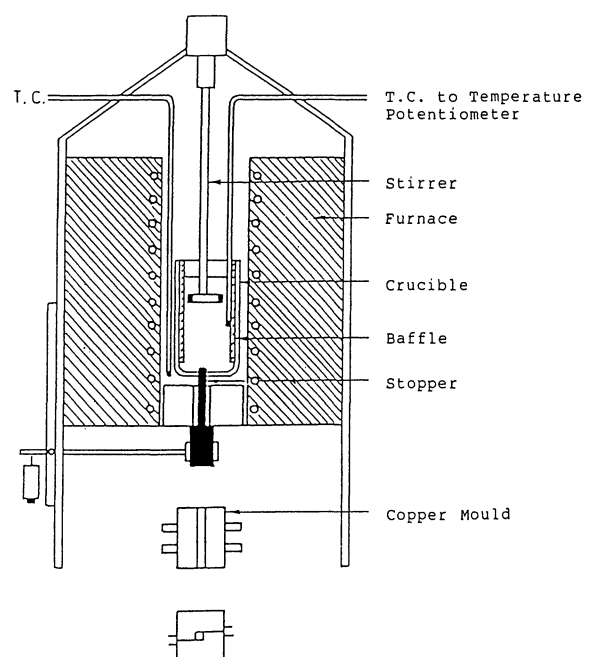


Fig. 1 Schematic experimental set up.

graphite crucible kept in a kanthal wound vertical muffle furnace. When the metal was heated to 1173 K, the deoxidizers were added to molten aluminium. Preheated ceramic coated baffles were pushed into the melt. The desired quantity of lead shots were added through an aluminium hopper and the melt was agitated with a four-bladed flat impeller of size $20 \times 10 \text{ mm}^2$ blade size at the rotational speed of 53 s^{-1} . Meanwhile the furnace was allowed to cool down naturally. When the temperature reached 973 K, the graphite stopper plugged at the bottom of the crucible was removed and the turbulent melt was poured into the copper mould surrounded by ice-brine. Castings were also taken at rotational speeds of 37 and 25 s^{-1} .

Specimens of stircast Al-Pb composites were taken

from different sections of the ingot and electropolished. The polished specimens were examined under Metavert optical microscope and particle size distribution was determined by Saltykova method⁽⁵⁾. Specimens were also studied under SEM to see the effect of lead content and rotational speed on the microstructure of the stircast Al-Pb composite.

III. Experimental Results and Discussion

1. Influence of composition on the microstructure of stircast Al-Pb composite

Figure 2(a) to (e) show the unetched SEM micrographs of stircast Al-Pb composite containing 3.69, 8.04, 10.39,

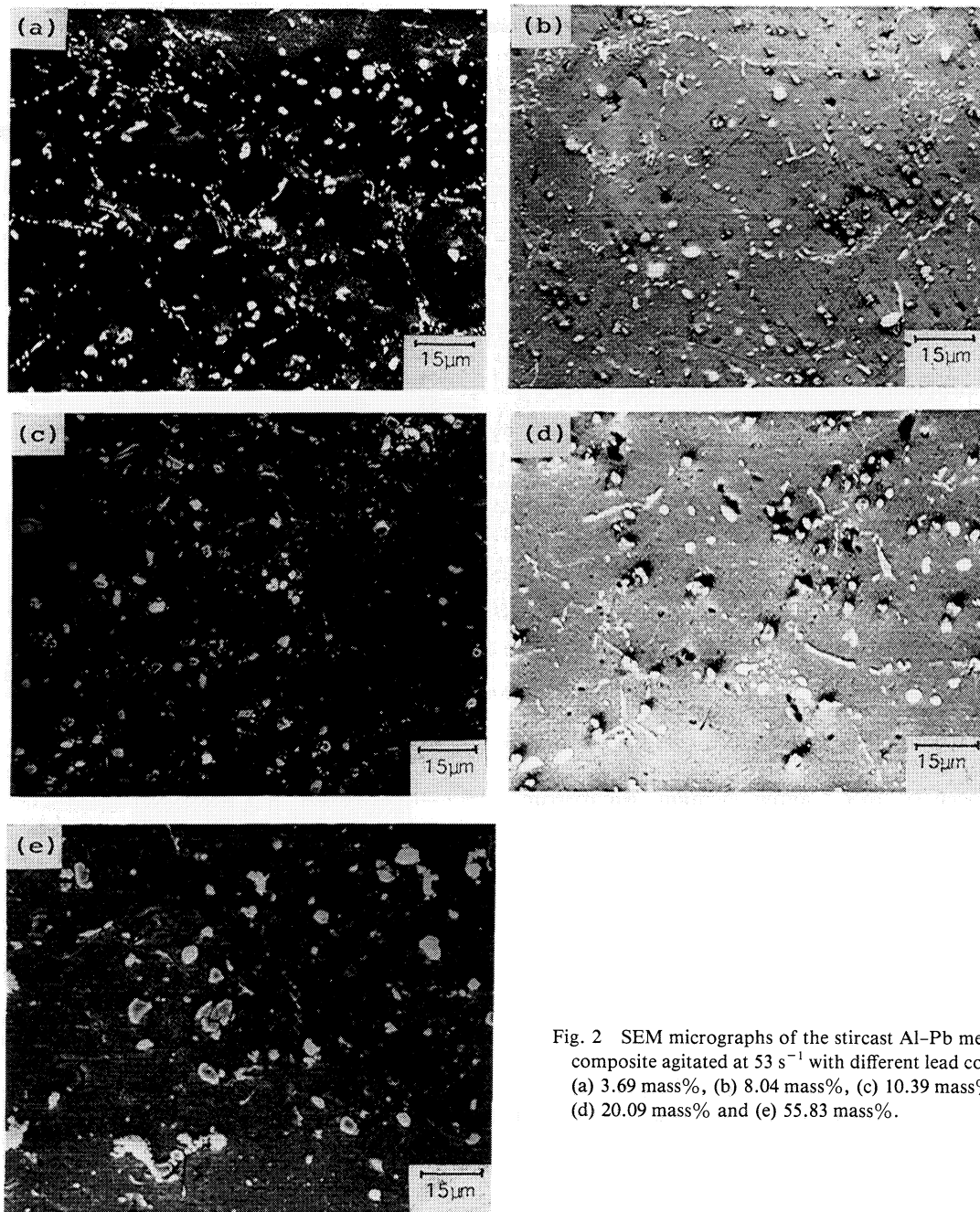


Fig. 2 SEM micrographs of the stircast Al-Pb metal-metal composite agitated at 53 s^{-1} with different lead contents of (a) 3.69 mass%, (b) 8.04 mass%, (c) 10.39 mass%, (d) 20.09 mass% and (e) 55.83 mass%.

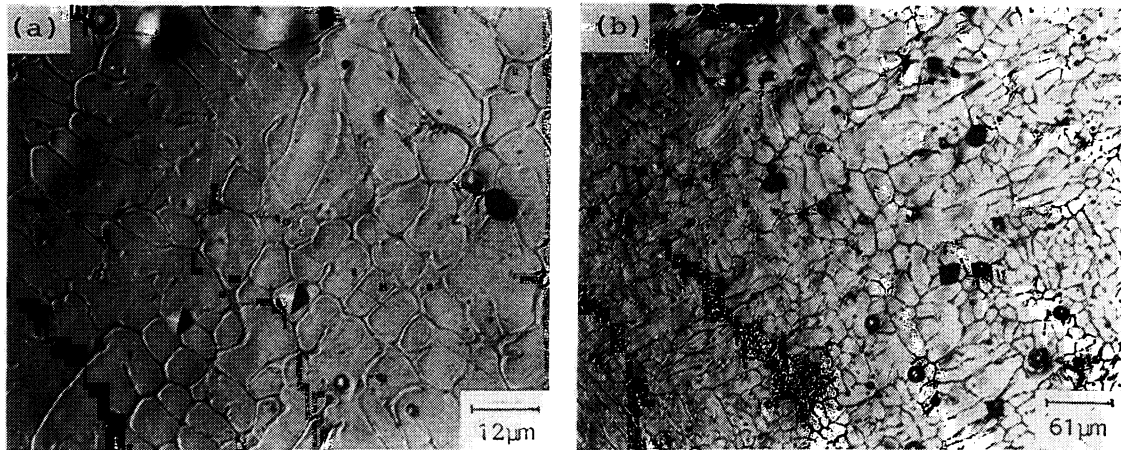


Fig. 3 Optical micrographs of stircast Al-Pb metal-metal composite with 9.2 mass% lead.

20.09 and 55.83 mass% lead, agitated at 53 s^{-1} . Lead rich particles (seen white) are uniformly distributed in the matrix of primary aluminium phase. All the white particles may not be lead-rich phase because alumina particles also will appear as white particles. At the boundaries of primary aluminium dendrite, AlFeSi needles are observed to form probably as a part of multicomponent eutectic in the last freezing liquid because of impurities in commercial aluminium. In case of Al-Pb composites with higher lead content, the spherical particles are seen to merge into each other giving elongated shapes of particles as seen in Fig. 2(e). Figure 3(a) and (b) show the etched microstructures of Al-Pb alloy with 9.2 mass% lead as observed under optical microscope. It is observed that some lead-rich particles are embedded in dendrites. The advancing dendrite front appear to have engulfed the liquid droplets of lead. It is also possible that these droplets may have nucleated on the solid aluminium-rich phase. Further, the white spot at the centre of the lead globules possibly indicates divorcing of eutectic. Lead content also influences the dendrite arm spacing of primary aluminium in stircast Al-Pb composite agitated at 53 s^{-1} . It has been observed that the spacing goes on decreasing with increase in lead content as revealed from Fig. 2(a) to (e) but it is not clear whether the droplets of lead-rich phase have any nucleating role resulting in refinement of dendrites.

2. Effect of stirring speed on the microstructure

The unetched microstructures of stircast Al-Pb composite containing 9.2 mass% lead but stirred during processing at different impeller speeds of 53, 37 and 25 s^{-1} , are shown respectively in Fig. 4(a) to (c). Microstructure consists of white particles of lead-rich phase whereas the matrix of primary aluminium is relatively dark.

Figure 4(a) reveals spherical particles of lead in stircast Al-Pb composite agitated at 53 s^{-1} and it has largest lead-rich particles of diameter $70 \mu\text{m}$ and smallest particles of diameter $4.5 \mu\text{m}$. Figure 4(b) reveals that particles of lead in composites stircast at 37 s^{-1} , are predominantly spherical but at places, the lead-rich par-

ticles appear to have joined. The largest particles of lead are of diameter $35 \mu\text{m}$ and the smallest ones are of $5 \mu\text{m}$. Figure 4(c) reveals that at 25 s^{-1} , the largest lead-rich particles are of diameter $28 \mu\text{m}$ and the smallest ones are of size $5.5 \mu\text{m}$. Thus, it is evident that the size range of particles reduces with decreasing agitator speed both due to sharp decrease in the size of largest particles and a slight increase in size of the smallest particles. Further, fine AlFeSi needles at the inter-dendritic region are observed along with oxide particles. The dendrite arms spacing is also influenced by agitator speed and it decreases with increase in agitator speed as revealed from Fig. 4(a) to (c).

3. Effect of lead content on particle size distribution

In stircast Al-Pb composite agitated at 53 s^{-1} with lead content varying from about 4 to 56 mass%, particle size of lead-rich phase ranges from 5 to $80 \mu\text{m}$. Figure 5 shows particle size distribution of stircast alloys containing around 10, 20 and 56 mass% lead, as characterised by variation of number of particles in terms of $\log N$, in a group of particles with a given mean diameter. It is observed that the number of particles in a given group increases with lead content. Figure 6 shows the variation in the percentage of larger lead-rich particles in the range of $60\text{--}80 \mu\text{m}$ with lead content in stircast Al-Pb alloys. It is revealed that the number percentage of larger lead-rich particles increases with increase in lead content. Inter-particles distance of lead-rich phase and dendrite arm spacing of primary aluminium phase have been observed to decrease with increase in lead content as shown in Figs. 7 and 8.

In liquid-liquid dispersion, with increase in amount of dispersed phase, probability of collisions of dispersed phase droplets increases which may result in formation of more large droplets by coalescence and these droplets remain in suspension under vigorous agitation in immiscible region. This phenomenon is evident from Figs. 5 and 6. The total number of particles also increases with increase in lead content as seen in Fig. 5 and results in decrease in inter-particle distance as shown in Fig. 7.

Vermeulen *et al.*⁽⁶⁾ observed in their study on liquid-

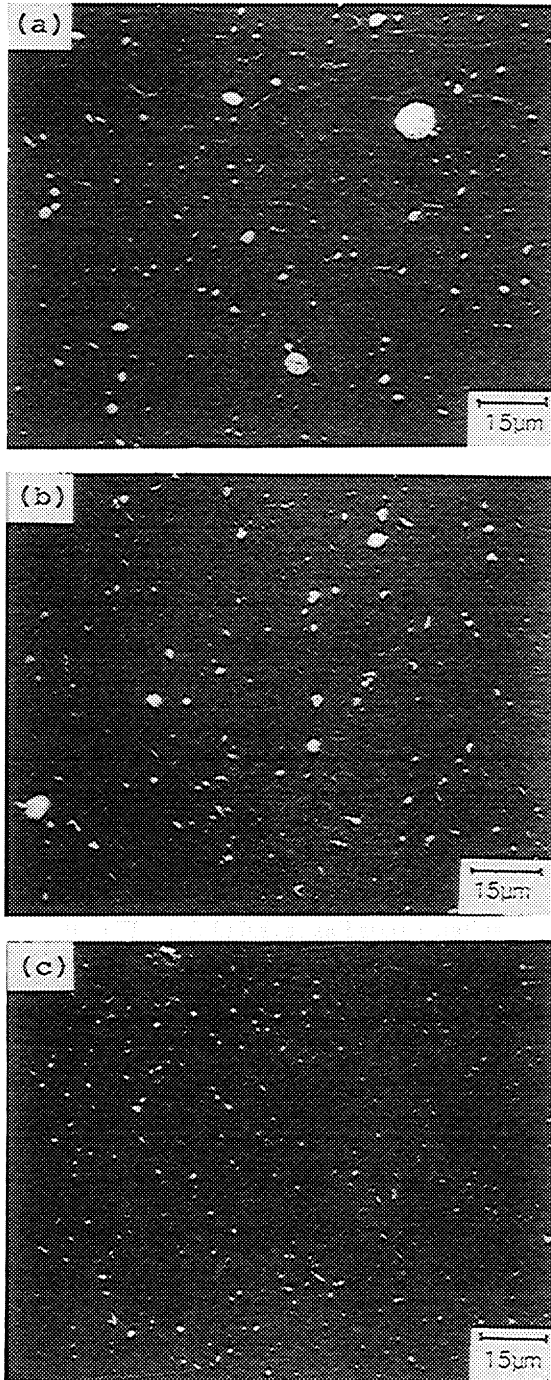


Fig. 4 SEM micrographs of stircast Al-Pb metal-metal composite with 9.2 mass% lead with different rotational speeds of (a) 53 s^{-1} , (b) 37 s^{-1} and (c) 25 s^{-1} .

liquid dispersion that the amount of dispersed phase affects the mean diameter of droplets dispersed, when the amount of the dispersed phase increases, the diameter of the droplets is also increased. However, one could not check as to whether the expression by Hinze⁽⁷⁾ or Nagata⁽⁸⁾ is correct as the maximum diameter could not be measured so precisely. But the number of particles in the largest size class increases with lead content as shown in Fig. 5. It appears that there is substance in the general argument that the overall dispersion obtained is the re-

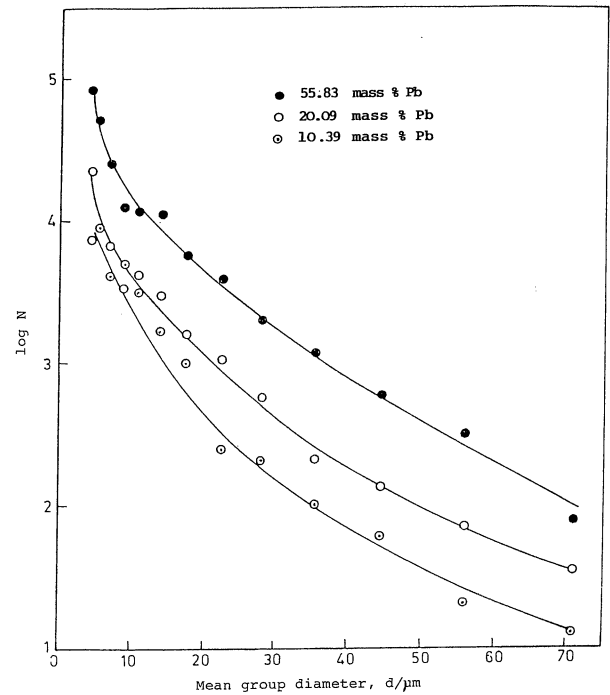


Fig. 5 Particle size distribution of stircast Al-Pb metal-metal composite with different lead content agitated at 53 s^{-1} .

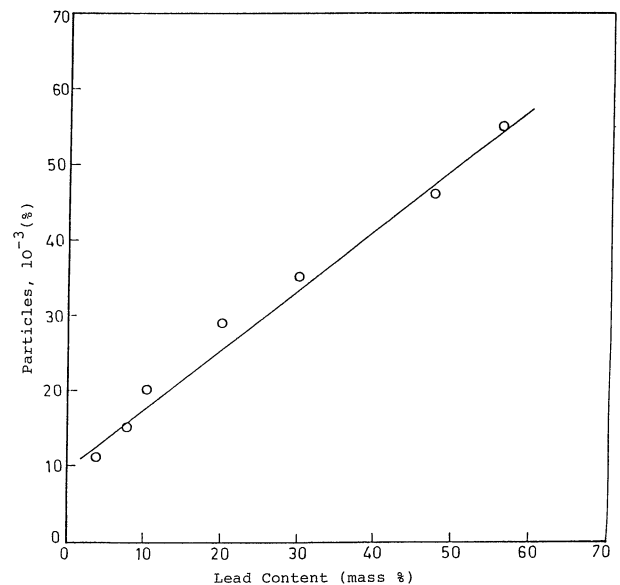


Fig. 6 The variation of number percentage of larger lead-rich particles with lead content in stircast Al-Pb metal-metal composites agitated at 53 s^{-1} .

sultant of two processes-(i) disintegration into droplets due to shear field and (ii) coalescence of droplets. The former reduces the size whereas the latter process enhances it. The observed size distribution displays the dynamic equilibrium between the two processes. Nagata⁽⁸⁾ has attributed the increase in size of dispersed droplets with an increase in dispersed phase to an enhanced coalescence and the observed size of the dispersed particles with an increase in lead content may also be attributed to the same process.

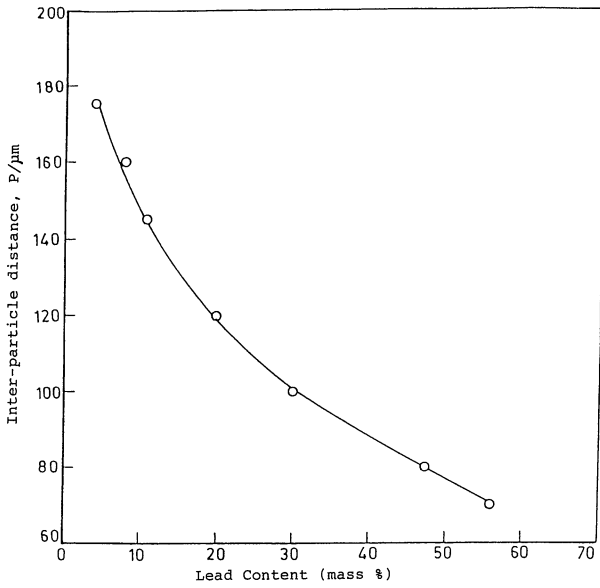


Fig. 7 The variation of inter lead-rich particle distance with lead content of stircast Al-Pb metal-metal composite agitated at 53 s^{-1} .

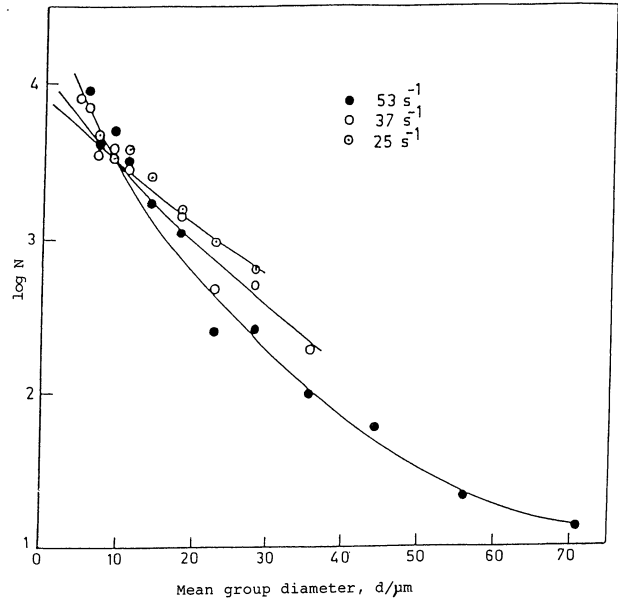


Fig. 9 Particle size distribution of stircast Al-9.2 mass%Pb metal-metal composites agitated at $53, 37$ and 25 s^{-1} .

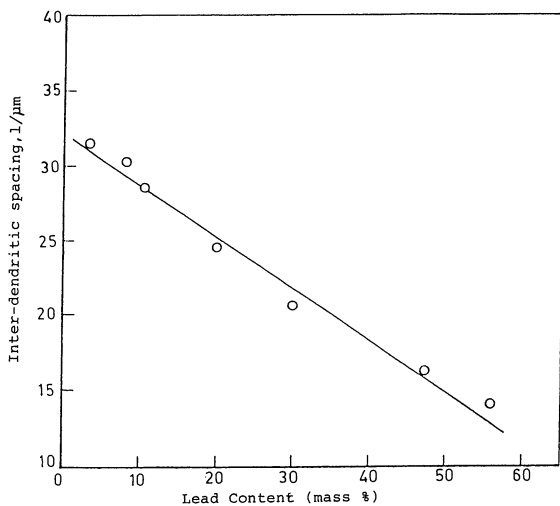


Fig. 8 The variation of dendrite arm spacing with lead content of stircast Al-Pb metal-metal composites agitated at 53 s^{-1} .

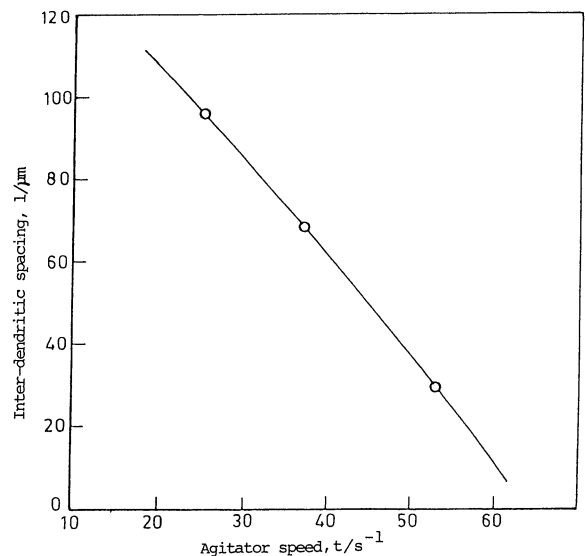


Fig. 10 The variation of dendrite arm spacing with agitator speed of stircast Al-9.2 mass%Pb metal-metal composites.

4. Effect of agitator speed on particle size distribution

The particle size distribution of lead-rich particles in stircast Al-Pb composite agitated at $53, 37$ and 25 s^{-1} with 9.2 mass\% lead has been determined by quantitative metallography. Figure 9 shows logarithmic variation of number of particles, $\log N$, with its mean group diameter at different agitator speeds. Figure 4(a), (b) and (c) show the SEM micrographs of stircast Al-Pb composite at the same agitator speeds. It is observed that the stircast composite agitated at 53 s^{-1} has the largest range of particle size from about $70 \mu\text{m}$ to $4.5 \mu\text{m}$. With a decrease in speed of agitation to 37 s^{-1} and 25 s^{-1} , the size range is reduced. It has also been observed that the number of particles of intermediate size between 20 to $30 \mu\text{m}$ are

increased with a decrease in agitator speed. Figure 10 shows the variation of dendrite arm spacing with agitator speed and it is observed that it decreases with an increase in agitator speed.

The aluminium being lighter phase, has been charged first in the crucible and solid lead shots are charged from the top while agitating molten aluminium vigorously with the help of a stirrer of size recommended by Nagata⁽⁸⁾ and following the practice recommended by Oldshue⁽⁹⁾ where lighter liquid is first charged and the heavier liquid is poured from the top while agitating.

Nagata *et al.*⁽⁸⁾ has also observed that in liquid-liquid dispersion, the mean diameter of droplet is reduced with increase in agitator speed because of increase in tur-

bulence in the vicinity of agitator, resulting in a large number of smaller droplets. However, it has also been observed that size of the largest droplet which may remain suspended in the liquid also increases with increase in agitator speed⁽⁸⁾. Thus, the diameter of largest size particle increases and that of smallest particle decreases with the increase in agitator speed thereby extending the range of sizes of dispersed particles as observed in the present investigation.

Further, when agitated Al-Pb melt is cooled within the mould, monotectic reaction takes place at 931.5 K and aluminium-rich phase is first to solidify dendritically rejecting lead along its boundaries where droplets of lead-rich phase nucleate and grow. Now, on further cooling to 600 K, eutectic reaction takes place and lead-rich phase is solidified along with a small amount of aluminium-rich phase constituting together the eutectic. Needles of AlFeSi are also observed along the boundaries of aluminium-rich phase due to the presence of iron and silicon as impurities in commercially pure aluminium used for this investigation.

During solidification of dendrites, droplets of lead-rich phase encounter this dendritic solidification front. There has been no investigation so far on the interaction of droplets with dendritic solidification front. Microstructures shown in Fig. 2(a) to (e) and Fig. 4(a) to (c) clearly reveal a tendency for lead-rich droplets to segregate at the dendritic boundaries indicating that the solidification front has mostly pushed the lead-rich droplets to interdendritic region. However, in the etched microstructures generally one observes some large lead-rich droplets engulfed by the dendrites.

IV. Conclusions

Stirred Al-Pb composites containing different amounts of lead and stirred during processing at different agitator speeds have shown a range of particle size of lead-rich particles distributed in a matrix of primary aluminium phase. A study of microstructure and particle

size distribution results in the following conclusions:

(1) With increase in lead content lead-rich particles are seen to merge to form elongated particles resulting in higher number density of large particles in the size range of 60–80 μm . Inter-particle distance is observed to decrease with increase in lead content.

(2) Dendrite arms spacing of primary aluminium is observed to decrease with increase in lead content. It lies within a range of 15 to 33 μm .

(3) With an increase in agitator speed, the range of particle sizes are extended at both large as well as small size limits. With an agitator speed of 25 s^{-1} , lead-rich particles are of size between 5.5 to 28.2 μm but with an increase in agitator speed to 37 s^{-1} , the size range is extended from 5 to 35.5 μm and with a further increase in speed to 53 s^{-1} , particles of sizes 4.5 to 70 μm are observed.

(4) Dendrite arms spacing of primary aluminium is observed to decrease with increase in agitator speed.

Acknowledgement

Investigators are very much thankful to Department of Science and Technology, India for providing financial assistance.

REFERENCES

- (1) T. Ikeda and S. Nishi: *J. Japan Inst. Metals*, **46** (1985), 645.
- (2) P. K. Rohatgi, S. Ray and Y. Liu: *Proc. ASM Conf. on Tribology of Composite Materials*, ed. by P. K. Rohatgi, P. J. Blau and C. S. Yust, ASM, Metals Park, Ohio, (1990), p. 1.
- (3) S. Mohan, V. Agarwala and S. Ray: *Materials Science and Engineering*, **A144** (1991), 215.
- (4) K. Ichikawa and S. Ishizuka: *Trans. Japan Inst. Metals*, **28** (1987), 145.
- (5) R. T. Dehoff and F. N. Rhines: *Quantitative Microscopy*, Mat. Sci and Engg. Series, McGraw-Hill Book Co., NY (1968), p. 151.
- (6) T. Vermeulen, G. M. Williams and G. E. Langlois: *Chem. Engg. Prog*, **51** (1955), 85F.
- (7) J. O. Hinze: *A. I. Ch. E. J.*, **1** (1955), 289.
- (8) S. Nagata: *Mixing Principles and Applications*, John Wiley and Sons, NY (1975), p. 298.
- (9) J. Y. Oldshue: *Fluid Mixing Technology*, Chemical Engg., McGraw-Hill Book Co., NY (1983), p. 125.